Title

Sequential Treatment of Estrogen Deficient, Osteopenic Rats with Alendronate, Parathyroid Hormone (1–34), or Raloxifene Alters Cortical Bone Mineral and Matrix Composition

Journal

Calcified Tissue International, 106(3)

ISSN

0171-967X

Authors

Taylor, Erik A
Donnelly, Eve
Yao, Xiaomei
et al.

Publication Date

2020-03-01

DOI

10.1007/s00223-019-00634-w

Peer reviewed

Calcified Tissue International (2020) 106:303–314
https://doi.org/10.1007/s00223-019-00634-w

ORIGINAL RESEARCH

Sequential Treatment of Estrogen Deficient, Osteopenic Rats with Alendronate, Parathyroid Hormone (1–34), or Raloxifene Alters Cortical Bone Mineral and Matrix Composition

Erik A. Taylor[1] · Eve Donnelly[2,3] · Xiaomei Yao[4] · Mark L. Johnson[4] · Sarah K. Amugongo[5] · Donald B. Kimmel[6] · Nancy E. Lane[5,7]

Received: 29 August 2019 / Accepted: 11 November 2019 / Published online: 29 November 2019

Abstract

Anti-resorptive and anabolic treatments can be used sequentially to treat osteoporosis, but their effects on bone composition are incompletely understood. Osteocytes may influence bone tissue composition with sequential therapies because bisphosphonates diffuse into the canalicular network and anabolic treatments increase osteocyte lacunar size. Cortical bone composition of osteopenic, ovariectomized (OVX) rats was compared to that of Sham-operated rats and OVX rats given monotherapy or sequential regimens of single approved anti-osteoporosis medications. Adult female Sprague–Dawley rats were OVX ($N=37$) or Sham–OVXd ($N=6$). After 2 months, seven groups of OVX rats were given three consecutive 3-month periods of treatment with vehicle (V), h-PTH (1–34) (P), alendronate (A), or raloxifene (R), using the following orders: VVV, PVV, RRR, RPR, AAA, AVA, and APA. Compositional properties around osteocyte lacunae of the left tibial cortex were assessed from Raman spectra in perilacunar and non-perilacunar bone matrix regions. Sequential treatments involving parathyroid hormone (PTH) caused lower mean collagen maturity relative to monotherapies. Mean mineral:matrix ratio was 2.2% greater, mean collagen maturity was 1.4% greater, and mean carbonate:phosphate ratio was 2.2% lower in the perilacunar than in the non-perilacunar bone matrix region (all $P<0.05$). These data demonstrate cortical bone tissue composition differences around osteocytes caused by sequential treatment with anti-osteoporosis medications. We speculate that the region-specific differences demonstrate the ability of osteocytes to alter bone tissue composition adjacent to lacunae.

Keywords Raman spectroscopy · Mineral:matrix · Carbonate:phosphate · Crystallinity · Collagen maturity · Osteocyte · Perilacunar

Electronic supplementary material The online version of this article (https://doi.org/10.1007/s00223-019-00634-w) contains supplementary material, which is available to authorized users.

✉ Nancy E. Lane
nelane@ucdavis.edu

[1] Sibley School of Mechanical and Aerospace Engineering, Cornell University, Ithaca, NY, USA

[2] Department of Materials Science and Engineering, Cornell University, Ithaca, NY, USA

[3] Research Division, Hospital for Special Surgery, New York, NY, USA

[4] Department of Oral and Craniofacial Sciences, School of Dentistry, University of Missouri-Kansas City, Kansas City, MO, USA

[5] Center for Musculoskeletal Health, University of California Davis Medical Center, Sacramento, CA, USA

[6] Department of Physiological Sciences, University of Florida, Gainesville, FL, USA

[7] Health Center, University of California At Davis, 4625 Second Avenue, Suite 2006, Sacramento, CA 95817, USA

Introduction

Osteoporosis is characterized by low bone mass and increased risk of fracture. Current approved treatments include both anti-resorptive and anabolic agents, such as parathyroid hormone (PTH), abaloparatide and romosozumab. The association of these treatments with improved bone mineral density (BMD) and bone quality, and the mechanisms by which they reduce risk of spine and hip fracture, has come under intense study. Strong anti-resorptives, like bisphosphonates (BPs), reduce bone resorption and formation, while increasing cortical thickness, cortical area, and cortical strength [1]. When combined, these effects may explain the reduction in fracture risk [2]. In contrast, PTH increases bone resorption and formation, while increasing cortical thickness, cortical area, and cortical strength [3]. The reduction in fracture risk, despite the opposite tissue level effects of anti-resorptives and PTH on bone resorption and bone formation, has motivated the use of sequential therapies with the two types of agents with the goal of producing better results than with either monotherapy. Preclinical studies have demonstrated that sequential anti-resorptive and anabolic therapies improve trabecular bone mass, microarchitecture, and strength, as well as cortical area, thickness, and strength [4, 5]. Clinical studies in osteoporotic patients given sequential anti-resorptive and anabolic therapies show that bone formation markers and spine and hip BMD improve more than with either monotherapy [2]. Although the effects of sequential anti-resorptive and anabolic therapies on the mechanical and microarchitectural properties of bone have been investigated, the effects of such sequential therapy on bone tissue composition at the collagen and mineral level are unknown.

Approaches to studying mineral and/or collagen in bone tissue include scanning electron microscopy (SEM), nanoindentation, synchrotron X-ray computed microtomography, Fourier transform infrared (FTIR) spectroscopy, and Raman spectroscopy (RS). FTIR and RS quantify bone composition by calculating peak area and intensity ratios representing vibrational modes specific to mineral and collagen. The primary endpoints measured by FTIR and RS are mineral:matrix ratio, representing the extent of collagen mineralization; carbonate:phosphate ratio, representing the extent of carbonate substitution into the hydroxyapatite crystal lattice; crystallinity, representing hydroxyapatite crystal size and stoichiometric perfection; and collagen maturity, representing the ratio of mature trivalent to immature divalent crosslinks [6].

Strong anti-resorptives reduce bone turnover and increase non-enzymatic crosslinking of the collagen matrix [7]. Bone structural units (BSUs) accumulate mineral throughout their lifespan. The reduced turnover rate caused by anti-resorptives increases the lifespan of individual BSUs, prolonging the time during which they accumulate mineral, causing them to reach a higher level of mineralization than is seen at normal turnover rates [8]. Alendronate, a strong anti-resorptive, alters bone quality in postmenopausal women by changing bone mineral properties, modulus, and microhardness [9]. Synchrotron small-angle X-ray scattering and wide-angle X-ray diffraction, FTIR spectroscopy, and advanced glycation end-products (AGEs) assessment of cortical bone tissue showed increased non-enzymatic crosslinking of the collagen matrix in alendronate-treated female dogs [7]. Mild anti-resorptive agents like raloxifene also appear to increase bone matrix mineralization [10]. In summary, anti-resorptives increase tissue mineral content, decrease crystallinity, and increase non-enzymatic crosslinking. In contrast, PTH appears to decrease crystallinity, collagen maturity [11], and AGEs [12]. Like their complementary effects on turnover, the complementary effects of anti-resorptives and PTH on bone tissue composition suggest that sequential therapy with anti-resorptive and anabolic agents may yield bone quality superior to either monotherapy alone.

Changes in whole-bone cross-sectional geometry, trabecular morphology, and tissue mechanical properties with anti-resorptive and anabolic therapies may also alter mechanical signals detected by osteocytes, which could then alter their surrounding matrix in an adaptive response to their new mechanical environment. Structural changes with anti-resorptive and anabolic treatment in cortical and trabecular compartments alter whole-bone stiffness and distribution of loads between compartments, thereby altering the macroscopic strains in the bone [13]. In addition to changing bone composition through their influence on bone turnover, bone-active agents may also alter tissue hardness and modulus by changing the microscopic mechanical environment in bone tissue near the osteocyte [9]. Young's modulus of bone tissue near osteocyte lacunae is lower than in more distant bone tissue [14]. Previous studies report changes in osteocytes of rats given continuous PTH [15], and in bone tissue composition surrounding osteocytes with intermittent PTH [16], along with diffusion of BPs into the canalicular network [17]. It is well-documented that osteocytes are capable of removing and replacing the perilacunar bone matrix during lactation [18–20]. These results suggest that osteocytes alter the properties of their surrounding tissue, a process which may be influenced by sequential anti-resorptive and anabolic therapies. Therefore, therapy-related changes to both bone structure and tissue mechanical properties may occur, altering mechanical signals perceived by osteocytes [21].

We hypothesize that sequential anti-resorptive and anabolic therapy in estrogen deficient, osteopenic rats alters

bone matrix composition adjacent to and far from osteocyte lacunae through its actions on osteocytes. When planning to study the effects of osteocytes on bone matrix composition, one must recall that bone remodeling is a process that affects bone matrix composition by altering tissue age. Thus, to obtain the clearest possible data about osteocyte effects on bone matrix composition, it would be advantageous to study bone tissue that is not influenced by bone remodeling. Since cortical bone in the rat long bone experiences no Haversian remodeling, we chose to study two bone matrix regions surrounding osteocytes (perilacunar and non-perilacunar bone matrix) in the central long bone cortex. The objectives of this study were to determine: (1) the effect of treatments on cortical bone tissue composition by comparing the mineral and collagen matrix properties in adult, osteopenic, ovariectomized (OVX) rats given sequential or monotherapy with anti-resorptive agents and PTH; and (2) whether treatment differentially affects composition within the cortex by comparing the mineral and collagen matrix properties in the perilacunar and non-perilacunar bone matrix regions.

Materials and Methods

Animals and Experimental Procedures

The bones examined here are a randomly selected subset of those from a previously reported experiment [4, 5]. Six-month-old female OVX ($N=37$) or Sham-operated Sprague–Dawley rats ($N=6$) were purchased from Harlan Laboratories (Livermore, CA, USA). The study protocol was approved by the University of California Davis Institutional Animal Care and Use Committee.

All OVX rats were allowed to develop trabecular osteopenia of the distal femur and lumbar vertebral body for 8 weeks, then randomized into seven groups that represent traditional long-term osteoporosis monotherapies or real-world osteoporosis therapies that begin with frontline anti-resorptive therapy that switches to either anabolic therapy or a drug holiday and then returns to the initial anti-resorptive therapy. For 90 days (Period 1), OVX rats were treated with either: (a) vehicle (V, normal saline), 1 ml/kg/dose, three times per week by subcutaneous (SC) injection (Life Technologies); (b) parathyroid hormone [P, h-PTH (1–34) (human) acetate], 25 µg/kg/dose, 5×/week SC (Bachem Biosciences, Inc., Torrance, CA, USA); (c) alendronate [A, 25 µg/kg/dose, 2×/week SC (Sigma-Aldrich Corp., St. Louis, MO, USA)]; or (d) raloxifene [R, 5 mg/kg/dose, 3×/week by oral gavage (Sigma-Aldrich Corp., St. Louis, MO, USA)]. After Period 1, rats were switched to their second treatment regimen. After a total of 180 days (end of Period 2), rats were switched to their third treatment regimen (Period 3). After a total of 270 days (end of Period 3), corresponding to ~ 4–6 years of treatment in humans (6 trabecular bone remodeling cycles), all rats were euthanized by CO_2 inhalation and necropsied. The groups are designated by the initial (V, P, A, or R) of the treatment applied during each period: VVV, PVV, RRR, RPR, AAA, AVA, and APA. Each treatment period involved only monotherapy. No two treatments were ever given simultaneously, meaning that combination treatment never occurred. Following euthanasia, the left tibiae were dissected free, wrapped in saline-soaked gauze, and frozen at − 20 °C. The number of samples from each group is in parentheses: VVV ($N=7$), PVV ($N=5$), RRR ($N=5$), RPR ($N=5$), AAA ($N=5$), AVA ($N=5$), and APA ($N=5$).

Raman Spectroscopy Analysis

A uniform specimen of 1.5 mm thickness was prepared from the proximal one-third of each left tibia (Fig. 1a), by making two parallel frontal plane cuts with a low-speed bone saw (Isomet; Buehler Co., Lake Bluff, IL, USA). The posterior face of the 1.5 mm section was polished under water with 1200 grit SiC paper to create a smooth surface and then ultrasonicated in deionized water to remove all debris. The section was mounted in a Petri dish with the anterior surface facing down. For RS, the Petri dish was filled with deionized water to submerge the specimen, and RS measurements of bone tissue surrounding osteocyte lacuna located in the central one-third region (relative to the periosteal and endocortical surfaces) of the lateral cortex 8–12 mm from the proximal end of the tibia were carried out (blue rectangle, Fig. 1a).

Raman spectra were collected in 1 µm increments along a linear path beginning ~ 1 µm from the lacunar wall and ending 20 µm from the lacunar wall (Fig. 1b). Raman linear scans were performed on both the right and left side of osteocyte lacunae, and four to five osteocyte lacunae were investigated for each rat. Care was taken to be sure that no portion of any linear path passed within 20 µm of a neighboring lacuna. Raman spectra were separated into two bone matrix regions as previously reported: (1) the perilacunar region (1–5 µm from the lacunar wall) [14, 16, 22]; and (2) the non-perilacunar region (16–20 µm from the lacunar wall) [14]. Thus, 40–50 Raman spectra were collected from each rat in each tissue region.

Spectra were obtained using a Raman microscope (LabRam HR 800 Horiba JobinYvon), with a helium–neon laser (633 nm) and a 60× water immersion objective (NA = 0.9; Olympus). Raman spectra (Fig. 1c) and were collected over the range 800–1800 cm^{-1} with a spectral resolution of 0.25 cm^{-1} and spatial resolution of ~ 1.5 µm with 90 s acquisition times. All subsequent spectral analysis was performed using custom code (Matlab, The Mathworks, Inc., Natick, MA, USA). Each spectrum was background

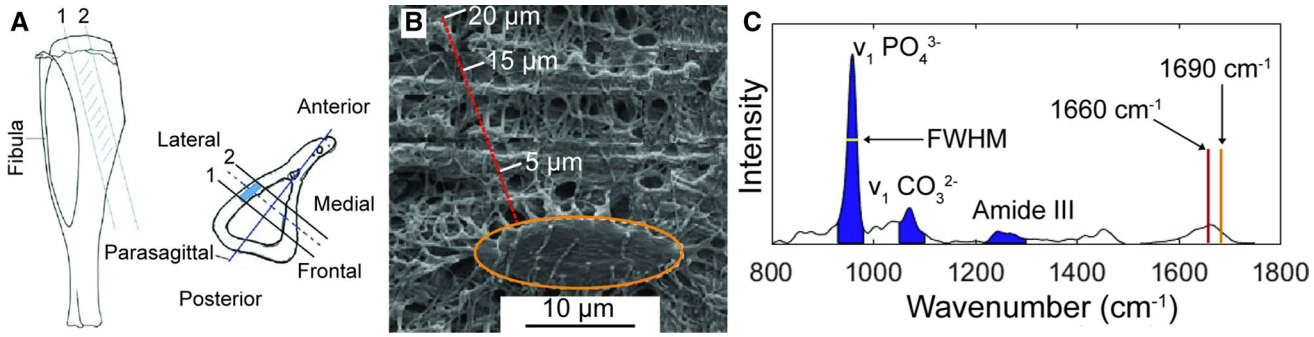

Fig. 1 Whole-bone and tissue level regions investigated by Raman spectroscopy (RS). **a** A 1.5-mm- thick section (hatched area) was removed from the proximal one-third of the tibia, by making two parallel frontal plane cuts (labeled 1 and 2). Spectra were collected from the central half of the lateral cortex 8–12 mm from the proximal end of the tibia (blue rectangle). **b** SEM image of an osteocyte lacuna (orange oval) and surrounding bone, showing a 20-µm-long linear RS measurement path (red dotted line, upper left). The third perpendicular line on the path is 20 µm from the lacunar wall. Five evenly spaced measurements were made at 1–5 µm from the lacunar wall (perilacunar region) and at 16–20 µm from the lacunar wall (non-perilacunar bone matrix region). **c** Representative Raman spectrum of rat cortical bone with the relevant mineral peak areas (ν_1 PO_4^{3-} and ν_1 CO_3^{2-}) and matrix peak area (amide III) shown in blue, the ν_1 PO_4^{3-} peak FWHM shown as a yellow horizontal line, and the peak intensities at 1660 cm^{-1} and 1690 cm^{-1} shown in red and orange, respectively

subtracted, baseline corrected, and normalized against the maximum intensity of the δ CH_2 peak (1446 cm^{-1}) [23].

Raman spectra were analyzed to determine the following endpoints: mineral:matrix ratio, carbonate:phosphate ratio, collagen maturity, and mineral crystallinity [23]. Integrated areas of the mineral ν_1 PO_4^{3-} (930–980 cm^{-1}) and $\nu_1 CO_3^{2-}$ (1050–1100 cm^{-1}) peaks, and the collagen matrix amide III peak (1250–1300 cm^{-1}) were calculated [24, 25] along with the intensities of the collagen matrix amide I peak at 1660 cm^{-1} and 1690 cm^{-1}. The mineral:matrix ratio was calculated as the peak area ratio of ν_1 PO_4^{3-}/amide III [6]. The carbonate:phosphate ratio was calculated as the peak area ratio of ν_1 $PO_4^{3-}/\nu_1 CO_3^{2-}$. Crystallinity was calculated as the inverse of the full width at half-maximum (FWHM) intensity of the ν_1 PO_4^{3-} peak at 960 cm^{-1}. Collagen maturity, recently validated with high performance liquid chromatography [26], was calculated from the intensity ratio of amide I peaks of 1660 cm^{-1} and 1690 cm^{-1}. For each rat, mean Raman parameters were calculated for each tissue region.

To examine the spatial variation of bone tissue composition for each rat, the FWHM of the distribution of each Raman endpoint, from spectra within tissue of the same region (perilacunar and non-perilacunar bone matrix) was calculated for each rat and combined to generate histograms of all four Raman parameters. The FWHM of the Gaussian curve fit to the endpoint distribution was used to assess compositional heterogeneity (Supplemental Fig. 1).

Statistical Analysis

Mean Raman outcomes were analyzed using a linear mixed model with (1) fixed effects of treatment and bone region (perilacunar and non-perilacunar) and the interaction between treatment and region; and (2) a random effect of rat to account for multiple spectra collected within each animal. Multiple comparisons were performed for the fixed effects of treatment and region using a Tukey post-hoc test with a Tukey correction for multiple comparisons. All values are expressed as mean ± SD. A significance level of $P < 0.05$ was used for all analyses.

Results

Effect of Treatment on Bone Tissue Composition

Tissue properties of the Sham group did not differ from those of the OVX group (VVV, Fig. 2a–d). Mean collagen maturity of the combined perilacunar and bone matrix regions was greater in rats treated with raloxifene monotherapy than in OVX (VVV, RRR + 12.4% vs. VVV; $P < 0.01$, Fig. 2d). Mean crystallinity was lower in rats given RPR sequential therapy versus OVX (VVV, RPR − 1.7% vs. VVV; $P < 0.01$, Fig. 2c).

Overall, sequential treatment with an anti-resorptive followed by PTH followed by an anti-resorptive lowered collagen maturity relative to monotherapy. Mean collagen maturity was lower in rats given sequential therapy that included alendronate followed by PTH followed by alendronate than with alendronate monotherapy (APA − 11% vs. AAA, $P = 0.02$, Fig. 2d). Mean collagen maturity was also lower in rats given sequential therapy that included raloxifene followed by PTH followed by raloxifene versus raloxifene monotherapy (RPR − 8.5% vs. RRR, $P = 0.03$, Fig. 2d). Furthermore, APA rats had lower collagen maturity relative

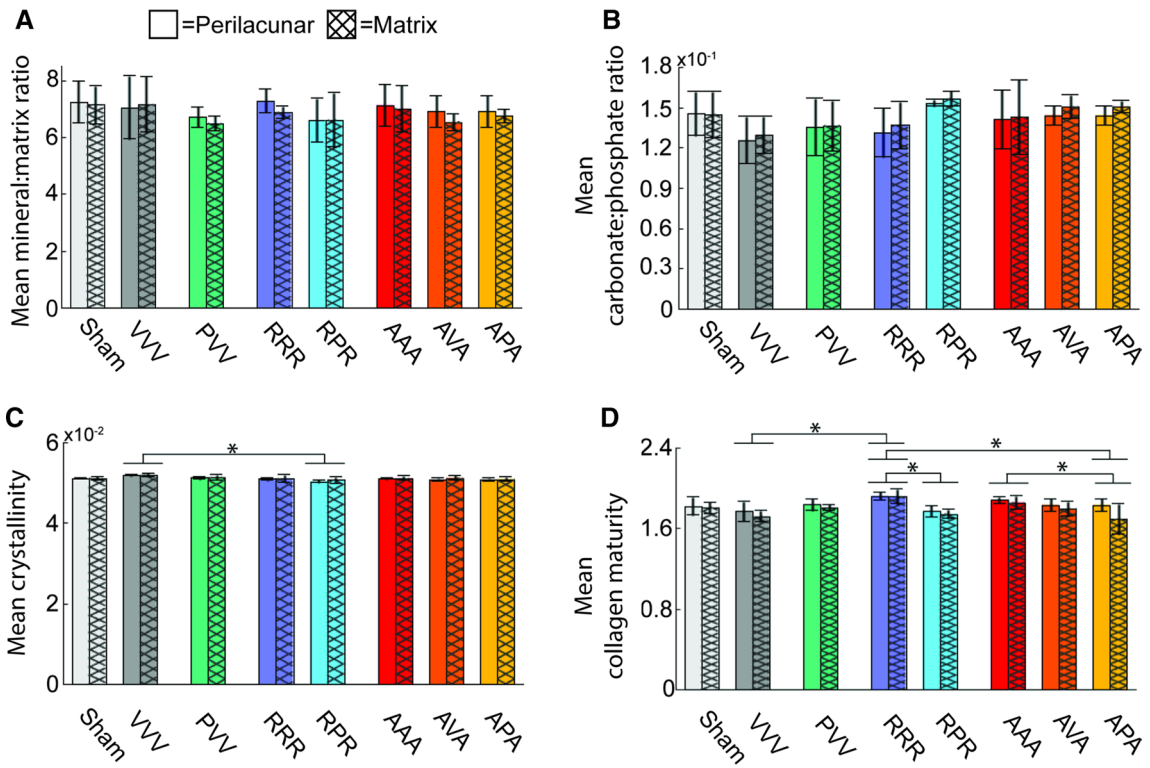

Fig. 2 Mean Raman spectroscopic parameters demonstrating the fixed effect of treatment, separated by treatments. The mineral:matrix ratio (**a**), carbonate:phosphate ratio (**b**), mineral crystallinity (**c**), and collagen maturity (**d**) are plotted. **P*0.05. Bar heights and error bars indicate mean ± SD, respectively. *VVV* vehicle–vehicle–vehicle, *PVV* PTH–vehicle–vehicle, *RRR* raloxifene–raloxifene–raloxifene, *RPR* raloxifene–PTH–raloxifene, *AAA* alendronate–alendronate–alendronate, *AVA* alendronate–vehicle–alendronate, *APA* alendronate–PTH–alendronate. Perilacunar region = open box and non-perilacunar bone matrix region = hatched box. See Supplemental Table 1 for *P*-values and percentage differences

to RRR monotherapy (− 12%, $P < 0.01$, Fig. 2d). Finally, sequential treatment altered the distributions of collagen maturity in a subset of treatment groups (see Supplemental Material).

Effect of Treatment on Distribution of Collagen Maturity

The distribution of collagen maturity narrowed with RPR sequential treatment relative to RRR monotherapy (− 38%, $P = 0.02$, Fig. 3). Bone tissue from rats receiving APA treatment had a narrower distribution of collagen maturity than those receiving raloxifene monotherapy (− 44% vs. RRR, $P < 0.01$) and tended to have a narrower distribution of collagen maturity than those receiving PVV treatment (− 36% vs. PVV, $P = 0.09$, Fig. 3).

Effect of Tissue Region on Bone Tissue Composition

The composition of the perilacunar region differed from that of the non-perilacunar bone matrix region. Differences between the perilacunar and non-perilacunar regions represent differences across all treatment groups because no significant interactions between treatment and tissue region were observed for any endpoint. In the perilacunar region versus the non-perilacunar region, the mineral:matrix ratio was greater (+ 2.2%, $P = 0.04$; Fig. 4a) and collagen maturity was greater (+ 1.4%, $P < 0.01$; Fig. 4d). In the perilacunar region, the carbonate:phosphate ratio was lower (− 2.2%, $P < 0.01$, Fig. 4b) and crystallinity was lower (− 0.3%, $P < 0.01$, Fig. 4c).

Discussion

Current approved treatments for osteoporosis include anti-resorptive therapies that slow bone resorption and bone formation and anabolic therapies that stimulate bone formation. Both types of monotherapy reduce risk of osteoporotic fracture. While most studies have focused on bone mass and density, biomechanical, and/or architectural changes brought about by these agents, this study evaluated localized micro-scale measures of bone composition around osteocytes in non-remodeling bone that underlie the above macro-level

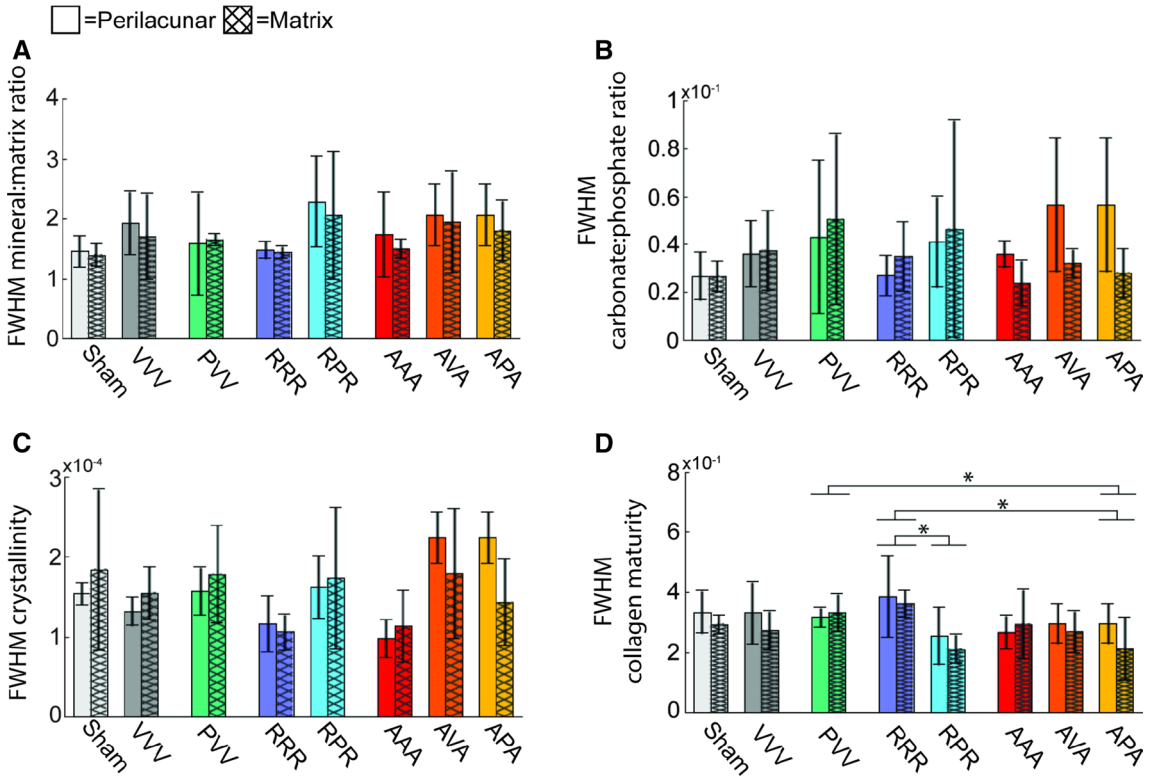

Fig. 3 Full width of half-maximum of the Gaussian fit to distributions of Raman spectroscopic parameters, separated by tissue region, including the **a** mineral:matrix ratio, **b** carbonate:phosphate ratio, **c** mineral crystallinity, and **d** collagen maturity. $^{*}P < 0.05$. Bar heights and error bars indicate mean ± SD, respectively. *VVV* vehicle–vehicle–vehicle, *PVV* PTH–vehicle–vehicle, *RRR* raloxifene–raloxifene–raloxifene, *RPR* raloxifene–PTH–raloxifene, *AAA* alendronate–alendronate–alendronate, *AVA* alendronate–vehicle–alendronate, *APA* alendronate–PTH–alendronate. Perilacunar region = open box and non-perilacunar bone matrix region = hatched box

measures. Our design and general type of measurements bear some similarity to recent publications [27, 28]. We treated osteopenic, OVX rats in three consecutive periods of three months each with different sequences of single osteoporosis treatment agents. We used RS to assess local bone chemistry surrounding osteocyte lacunae to determine differences in cortical bone material composition that could account for our previous observation that anti-resorptive therapies in combination with PTH result in higher bone mass and strength and better microarchitecture than any monotherapy [4, 5]. Sequential treatment with an anti-resorptive followed by PTH followed by the anti-resorptive produced lower collagen maturity relative to sequential monotherapies and lower mineral crystallinity relative to untreated OVX controls. The composition of the perilacunar region differed from that of the non-perilacunar bone matrix region. Based on these results and the a priori knowledge that osteocytes can remove and replace perilacunar mineral [14–16, 18–20], we speculate that sequential treatments with osteoporosis treatment agents cause osteocytes to alter bone tissue composition in their surrounding microenvironment to reduce collagen maturity without changing mineral:matrix ratio, carbonate:phosphate ratio, and crystallinity.

Effect of Treatment on Bone Tissue Composition

Sequential treatment with an anti-resorptive followed by PTH followed by an anti-resorptive predominantly affected the organic matrix phase, decreasing collagen maturity relative to monotherapy. Mean collagen maturity was lower with APA and RPR treatments versus their respective monotherapy. These results suggest that sequential treatments that involve PTH and anti-resorptive therapies lead to collagen with a lower ratio of mature trivalent crosslinks to immature divalent crosslinks [23, 29–32], consistent with stimulation of bone formation by PTH [2, 3]. This result is notable because it was obtained in cortical bone tissue that experiences no Haversian remodeling, raising the possibility that these therapies may cause osteocytes to change the composition of their surrounding bone independently of the bone age-related effects caused by differing turnover rates associated with use of anti-resorptive and anabolic treatments.

Mineral composition also differed with sequential anti-resorptive and anabolic treatments. Specifically, mean mineral crystallinity was 0.3% lower in rats given RPR sequential therapy than in OVX rats. This lower crystallinity corresponds to a decrease in hydroxyapatite crystal

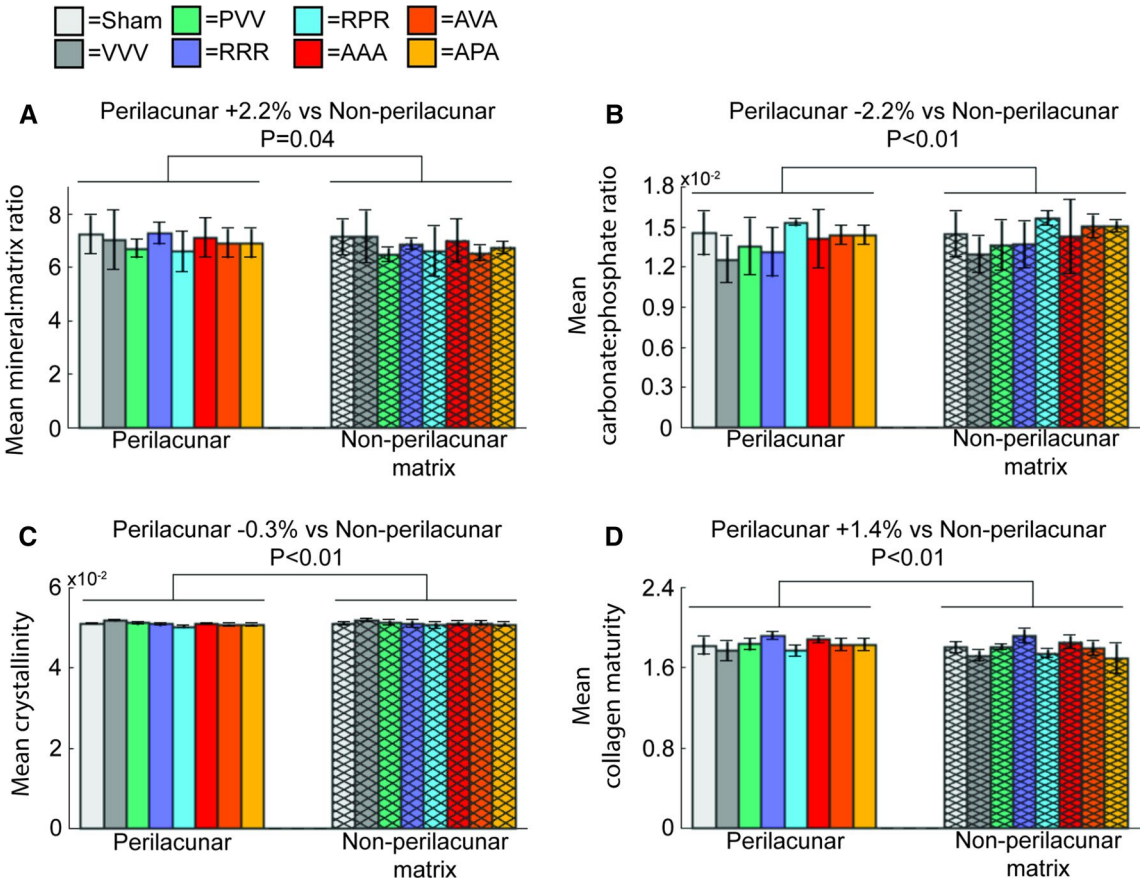

Fig. 4 Mean Raman spectroscopic parameters demonstrating the fixed effect of tissue region, separated by tissue region. The mineral:matrix ratio (**a**), carbonate:phosphate ratio (**b**), mineral crystallinity (**c**), and collagen maturity (**d**) are re-plotted (vs. Figure 2) to clarify the relationship of the perilacunar and non-perilacunar bone matrix regions. **P*0.05. Bar heights and error bars indicate mean ± SD, respectively. *VVV* vehicle–vehicle–vehicle, *PVV* PTH–vehicle–vehicle, *RRR* raloxifene–raloxifene–raloxifene, *RPR* raloxifene–PTH–raloxifene, *AAA* alendronate–alendronate–alendronate, *AVA* alendronate–vehicle–alendronate, *APA* alendronate–PTH–alendronate. Perilacunar region = open box, non-perilacunar bone matrix region = hatched box

size and stoichiometric perfection. This result is consistent with lower mineral crystallinity after PTH treatment [11, 33] and with maintained [34, 35] or lowered [9, 36] mineral crystallinity with anti-resorptive monotherapy. Additionally, raloxifene is known to increase matrix bound water content, which may play a role in the altered mineral crystallinity, although the exact nature of this interaction and the direction of the effect on crystallinity is unknown [37]. Despite these differences in mineral crystallinity, no differences were found in the mineral:matrix ratio, the extent of collagen mineralization, similar to results reported for anti-resorptive monotherapy [9]. The lower mineral crystallinity is most likely due to decreased stoichiometric perfection rather than decreased crystal size because the hydroxyapatite crystal width is correlated with tissue mineral content [38], and no differences in mineral:matrix ratio were observed [9]. This conclusion is further supported by the nominal increase in the carbonate:phosphate ratio in rats given RPR sequential therapy versus OVX controls because greater carbonate substitution into the crystal lattice decreases crystal size and stoichiometric perfection [39]. Again, this result is unique, because it was obtained in non-remodeling bone, and could make one speculate that these therapies cause osteocytes to change the composition of their surrounding bone.

It is well known that osteoporosis treatment agents can act through bone remodeling activity to change bone tissue composition [6, 34, 36, 40]. It is possible that tissue level mechanisms other than bone remodeling, such as osteocyte activity, exist, that may also respond to osteoporosis treatment agents by changing bone tissue composition. The effects of these additional tissue level mechanisms on bone tissue composition are impossible to separate from those caused by changes in the hormonal environment or agents mediated through bone remodeling activity. Thus, our measurements examine the effect of ovariectomy and osteoporosis treatment agents on bone tissue composition around osteocytes in *non-remodeling* cortical bone. If an osteoporosis treatment agent were to change bone tissue composition

in remodeling bone tissue, but not in non-remodeling tissue, one would not only know that it acts by affecting bone remodeling activity, but could also legitimately speculate that they it does not affect other tissue level mechanisms like osteocyte activity. Our data, like many [28, 41, 42], but not others [43], show no differences in composition of cortical bone between Sham–OVX and OVX rats. On the other hand, data from non-human primate cortical bone remodeling sites, show that bone tissue composition differs in OVX and Sham–OVX animals in a bone site where both remodeling activity and osteocyte activity are ongoing [44, 45]. Based on these data, it is apparent that estrogen deficiency accelerates bone remodeling activity and changes bone composition. However estrogen deficiency does not cause osteocyte activity to change bone composition in non-remodeling bone, leading one to consider the likelihood that bone remodeling activity, not osteocyte activity, is the tissue level mechanism through which estrogen deficiency affects bone tissue composition.

The combined results of our tissue level Raman compositional outcomes here with mechanical and microarchitectural measures on whole bones [5] show that sequential anti-resorptive and PTH therapies improve bone quality at multiple levels. Sequential anti-resorptive and PTH therapies decrease tissue age by promoting new bone formation, based on collagen maturity outcomes [46], while these therapies also produce and maintain better bone mass, microarchitecture, and strength than can be achieved by monotherapy [5]. Our data suggest that these therapies may also act by affecting bone composition around osteocytes.

Bone composition in rats that received PTH (1–34) during Period 1 or Period 2 still differs 90–180 days after the last exposure to PTH (1–34). Osteocyte lacunar size enlarges during lactation [47, 48] or PTH (1–34) treatment [15] within weeks and is maintained for the duration of the altered physiologic state. Few studies have provided data about bone composition after cessation of PTH (1–34). We speculate that after PTH (1–34) cessation, new mineralized tissue is deposited on the lacunar wall, reducing osteocyte lacunar size. Our data show that the bone tissue near osteocytes retains a different composition for up to six months after cessation of PTH (1–34).

Region-Specific Compositional Properties

A consequence of a heterogeneous distribution of composition within the bone tissue is a heterogeneous distribution of mechanical properties. At the cellular level, the osteocyte is believed to be the main mechanosensory cell in bone, orchestrating the actions of osteoclasts and osteoblasts in response to load-induced strain [49]. How the osteocyte perceives strain is largely unknown, but strain distributions within bone vary in a heterogeneous pattern, which are likely dependent upon the heterogeneous composition of bone [21]. One aspect of this heterogeneity is the bone tissue surrounding the osteocyte lacunae including perilacunar and non-perilacunar bone matrix regions, which play important roles in the strain environment experienced by the osteocyte [50]. These regions may be functionally distinct in that under certain conditions, such as during lactation [47], exercise [22], or PTH treatment [15, 16], the perilacunar region undergoes osteocyte-mediated remodeling, a localized process that does not affect the non-perilacunar bone matrix tissue region [18–20]. The elastic modulus of the perilacunar region differs from that in the non-perilacunar bone matrix region [14, 51], which modulates the strain fields experienced by osteocytes. Though we did not directly examine osteocytes for morphologic signs of treatment-related differences in activity, we speculate that the different bone composition outcomes following treatment may be an indicator of such activity. These studies, combined with our data, may indirectly suggest that bone tissue composition surrounding osteocytes is also altered by sequentially applied anti-resorptive and anabolic osteoporosis treatment medications.

The bone mineral composition of the perilacunar region differed from that of the non-perilacunar bone matrix region. The perilacunar region had greater mean mineral:matrix ratio, lower crystallinity, greater mean collagen maturity, and lower mean carbonate:phosphate ratio (Fig. 4b) compared to the non-perilacunar bone matrix region. These differences suggest that though the perilacunar tissue is more highly mineralized, the mineral is also more chemically pure with less carbonate substitution into the crystal lattice.

These results differ somewhat from those reported in a recent study on the effects of intermittent h-PTH (1–34) on bone tissue composition in the perilacunar and non-perilacunar bone matrix region in intact mice. In parallel with our results, the prior study found no significant interaction between tissue region and treatment on bone tissue composition. In contrast to our findings, the prior study found decreased mineral:matrix ratio in the perilacunar region compared to the non-perilacunar bone matrix region across both intermittent h-PTH (1–34) and vehicle treatments. Several factors could potentially contribute to the observed differences, including differing definitions of the non-perilacunar bone matrix region (10–15 m from the lacunar wall [16] vs. 16–20 m here), the estrogen deficient status of most of our groups, and intrinsic differences between the rat and mouse skeletons.

The greater tissue mineral content in the perilacunar region observed in the current study may reduce the ratio of globally applied strain to the local strain signal near the osteocyte. Differences in mineral and matrix properties between the perilacunar bone and non-perilacunar matrix suggest complex region-specific changes that may be associated with perilacunar osteocyte activity. The lower

carbonate:phosphate ratio in the perilacunar region vs. the non-perilacunar matrix indicates more recent nucleation of the mineral crystals and the possibility of increased perilacunar osteocyte activity [46]. In contrast, the greater relative concentration of mature trivalent crosslinks in the perilacunar region versus the non-perilacunar matrix indicates the presence of more mature collagen. Together these results mean that one could speculate that perilacunar osteocyte activity promotes turnover of the mineral crystals while allowing continued maturation of the collagen matrix [46].

Since we studied non-remodeling bone and made no direct studies of osteocytes, we speculate that the modest compositional differences seen here arise from the ability of osteocytes to alter their microenvironment [15, 18–20, 51]. The osteocyte microenvironment appears to influence predominantly the mineral phase of bone. Osteocytes add and remove mineral in the perilacunar bone [18–20, 51, 52]. Our results may provide additional evidence that osteocyte-based deposition and removal of mineral is more prominent in perilacunar bone matrix than in more distant bone matrix, because bone composition in the perilacunar bone matrix differs from that in the more distant bone matrix. The greater mineral:matrix ratio observed in the perilacunar region relative to the non-perilacunar bone matrix may arise from the specialized ability of the osteocyte to transfer calcium between the serum and the perilacunar region [52]. The lower carbonate:phosphate ratio in the perilacunar region is consistent with an acid phosphatase-mediated dissolution of the mineral phase in an acidic environment, because mineral acid phosphate content increases with decreased carbonate:phosphate ratio and pH [51]. The low carbonate:phosphate ratio is consistent with the increase in mineral solubility in the perilacunar region relative to the non-perilacunar bone matrix region and suggests the presence of newly formed mineral [52]. Although the 2.2% greater tissue mineral content in perilacunar bone appears inconsistent with the observation that the elastic modulus of the perilacunar tissue is 3–13% less than the non-perilacunar bone matrix in OVX rats, other aspects of bone composition could play a role. Specifically, the ability of an osteocyte to increase the size of canaliculi may increase the microporosity of bone tissue in the perilacunar region, which would decrease the indentation modulus, without altering the mineral:matrix ratio [48]. Both observations are consistent with a scenario in which the osteocyte creates a gradient of increasing tissue mineral content in the 20 μm of surrounding bone matrix.

These results suggest that incorporating PTH with raloxifene in sequential therapy produces bone tissue with a more spatially homogeneous ratio of mature trivalent crosslinks to immature divalent crosslinks. This result is consistent with previous reports that anti-resorptive monotherapy narrows the distributions of compositional properties [38, 40]. This result is unique, because it was obtained in non-remodeling bone, and appears to indicate that these therapies cause osteocytes to change the composition of their surrounding bone, an alteration that may be more difficult to detect in trabecular bone due to its higher remodeling rate.

The design of the experiment [4, 5] has a number of strengths that include evaluating the effect on bone mass and quality of sequential therapies with medications that have opposite tissue level mechanisms of action and are prescribed by clinicians to reduce fracture risk in postmenopausal women. In addition, we evaluated cortical bone from both anti-resorptive and anabolic sequential treatments using a rat model of estrogen deficiency osteopenia with trabecular bone behavior similar to that in women with postmenopausal osteoporosis [4]. We chose to evaluate cortical bone to limit the effect of local variations in tissue age that are apt to be more marked in trabecular bone than in cortical bone, due to the higher rate of remodeling in trabecular than cortical bone. Rat cortical bone is, for these measurements, likely to be a reasonable model for human cortical bone. Although it is often stated that rat long bone cortical bone *does not* remodel and human long bone cortical bone *does* remodel, implying that they are quite different, the absolute remodeling rates, 0% (or "not at all") in rats and 3% in humans [53, 54], are very similar. The overall interpretation is that cortical bone in the rat long bone, that resides in a species that lives two years as an adult, undergoes no remodeling during the two years of life, while human long bone cortical bone, that resides in a species that lives roughly 60 years as an adult, undergoes remodeling once every 30 years. Cortical bone in both species is thus very inactive. Therefore, our cortical bone measurements in rats are certain to represent bone tissue that has not been recently remodeled, and it is *highly likely* that cortical bone measurements from humans would also come from bone tissue that has not been recently remodeled. On this basis, the cortical bone composition measurements performed in these experiments have a good chance to be relevant to clinical studies.

However, there are also several weaknesses. We evaluated bone composition only after 270 days. Evaluating earlier samples may provide additional information about changes in the bone matrix caused by the individual treatments (e.g., immediately after cessation of PTH). In addition, we did not evaluate trabecular bone, due to its high rate of remodeling that could easily obscure effects on bone composition that are mediated through tissue level mechanisms other than remodeling activity, such as osteocyte activity and physiological changes in mineral metabolism. Finally, although we were certain of the distance of bone tissue from the osteocyte lacunar wall in the plane of the linear measurement path, it is not possible to know the location of any osteocyte lacunae that existed in the 10 μm of bone tissue that was

removed just adjacent to the plane of tissue that contained the linear paths.

In summary, we used RS to analyze differences in cortical bone matrix composition in female rats that had been treated with either monotherapies or sequential therapies with alendronate, raloxifene and/or h-PTH (1–34). We identified differences in the organic matrix composition with sequential therapies which may reflect differences in bone quality. Also, we identified compositional differences in the mineral and organic matrix phase surrounding osteocyte lacunae, potentially implicating osteocytes in altering the local tissue and treatments in changing that osteocyte activity. Additional studies of considerable interest include direct studies of osteocyte activity and how osteocytes' ability to perceive strain and how the propagation of microcracks change are related to changes in the composition of the perilacunar matrix. Additional studies with clinical cortical bone samples are warranted to determine if these results can be translated to inform health care providers about cortical bone quality changes in their patients treated sequentially with anti-resorptive and anabolic agents.

Acknowledgements We acknowledge Lynn Johnson, PhD, of the Cornell Statistical Consulting Unit for assistance with statistical analysis. This work was funded by National Institutes of Health Grants #'s R01 AR043052-07, 1 P50 AR03043, P50 AR060752NIH to NEL; The Endowment for Aging Research at UC Davis to NEL; and the Center for Musculoskeletal Health at UC Davis.

Compliance with Ethical Standards

Conflict of interest Erik A. Taylor, Eve Donnelly, Xiaomei Yao, Mark L. Johnson, Sarah K. Amugongo, Donald B. Kimmel, and Nancy E. Lane declare that they have no conflict of interest or disclosures.

Human and Animal Rights and Informed Consent We present no data from groups of human patients or individual human participants in this study. All applicable international, national, and institutional guidelines for the care and use of animals were followed. All procedures performed during studies involving animals were in accordance with the ethical standards of practice at the University of California, Davis. This study only reports data from animal experiments for which the statement on animal welfare is included.

References

1. Gasser JA, Ingold P, Venturiere A et al (2008) Long-term protective effects of zoledronic acid on cancellous and cortical bone in the ovariectomized rat. J Bone Miner Res 23:544–551. https://doi.org/10.1359/jbmr.071207
2. Cosman F (2014) Anabolic and antiresorptive therapy for osteoporosis: combination and sequential approaches. Curr Osteoporos Rep 12:385–395. https://doi.org/10.1007/s11914-014-0237-9
3. Mosekilde L, Danielsen CC, Søgaard CH et al (1995) The anabolic effects of parathyroid hormone on cortical bone mass, dimensions and strength-assessed in a sexually mature, ovariectomized rat model. Bone 16:223–230. https://doi.org/10.1016/8756-3282(94)00033-V
4. Amugongo SK, Yao W, Jia J et al (2014) Effects of sequential osteoporosis treatments on trabecular bone in adult rats with low bone mass. Osteoporos Int 25:1735–1750. https://doi.org/10.1007/s00198-014-2678-5
5. Amugongo S, Yao W, Jia J et al (2014) Effect of sequential treatments with alendronate, parathyroid hormone (1–34) and raloxifene on cortical bone mass and strength in ovariectomized rats. Bone 67:257–268. https://doi.org/10.1097/OPX.0b013e3182540562
6. Boskey A, Mendelsohn R (2005) Infrared analysis of bone in health and disease. J Biomed Opt 10:31102. https://doi.org/10.1117/1.1922927
7. Acevedo C, Bale H, Gludovatz B et al (2015) Alendronate treatment alters bone tissues at multiple structural levels in healthy canine cortical bone. Bone 81:352–363. https://doi.org/10.1016/j.bone.2015.08.002
8. Burr DB, Allen MR, Miller LM et al (2011) Bisphosphonates do not alter the rate of secondary mineralization. Bone 49:701–705. https://doi.org/10.1016/j.bone.2011.05.009
9. Bala Y, Depalle B, Farlay D et al (2012) Bone micromechanical properties are compromised during long-term alendronate therapy independently of mineralization. J Bone Miner Res 27:825–834. https://doi.org/10.1002/jbmr.1501
10. Burket JC, Brooks DJ, MacLeay JM et al (2013) Variations in nanomechanical properties and tissue composition within trabeculae from an ovine model of osteoporosis and treatment. Bone 52:326–336. https://doi.org/10.1016/j.bone.2012.10.018
11. Paschalis EP, Burr DB, Mendelsohn R et al (2003) Bone mineral and collagen quality in humeri of ovariectomized cynomolgus monkeys given rhPTH (1–34) for 18 months. J Bone Miner Res 18:769–775. https://doi.org/10.1359/jbmr.2003.18.4.769
12. Saito M, Marumo K, Kida Y et al (2011) Changes in the contents of enzymatic immature, mature, and non-enzymatic senescent cross-links of collagen after once-weekly treatment with h-PTH (1–34) for 18 months contribute to improvement of bone strength in OVX monkeys. Osteoporos Int 22:2373–2383. https://doi.org/10.1007/s00198-010-1454-4
13. Eswaran SK, Gupta A, Adams MF, Keaveny TM (2006) Cortical and trabecular load sharing in the human vertebral body. J Bone Miner Res 21:307–314. https://doi.org/10.1359/JBMR.051027
14. Stern A, Yao X, Wang Y et al (2018) Effect of osteoporosis treatment agents on the cortical bone osteocyte microenvironment in adult estrogen-deficient, osteopenic rats. Bone Rep 8:115–124. https://doi.org/10.1016/j.bonr.2018.02.005
15. Tazawa K, Hoshi K, Kawamoto S et al (2004) Osteocytic osteolysis observed in rats to which parathyroid hormone was continuously administered. J Bone Miner Metab 22:524–529. https://doi.org/10.1007/s00774-004-0519-x
16. Gardinier JD, Al-Omaishi S, Rostami N et al (2018) Examining the influence of PTH (1–34) on tissue strength and composition. Bone 117:130–137. https://doi.org/10.1016/j.bone.2018.09.019
17. Roelofs AJ, Stewart CA, Sun S et al (2012) Influence of bone affinity on the skeletal distribution of fluorescently labeled bisphosphonates in vivo. J Bone Miner Res 27:835–847. https://doi.org/10.1002/jbmr.1543
18. Wysolmerski JJ (2013) Osteocytes remove and replace perilacunar mineral during reproductive cycles. Bone 54(2):230–236. https://doi.org/10.1016/j.bone.2013.01.025
19. Qing H, Bonewald LF (2009) Osteocyte remodeling of the perilacunar and pericanalicular matrix. Int J Oral Sci 1(2):59–65. https://doi.org/10.4248/ijos.09019
20. Tsourdi E, Jähn K, Rauner M, Busse B, Bonewald LF (2018) Physiological and pathological osteocytic osteolysis. J Musculoskelet Neuronal Interact 18(3):292–303

21. Nicolella DP, Moravits DE, Gale AM et al (2006) Osteocyte lacunae tissue strain in cortical bone. J Biomech 39:1735–1743. https://doi.org/10.1016/j.jbiomech.2005.04.032
22. Gardinier JD, Al-Omaishi S, Morris MD, Kohn DH (2016) PTH signaling mediates perilacunar remodeling during exercise. Matrix Biol 52–54:162–175. https://doi.org/10.1016/j.matbio.2016.02.010
23. Mandair GS, Morris MD (2015) Contributions of Raman spectroscopy to the understanding of bone strength. BoneKEy 4:1–8. https://doi.org/10.1038/bonekey.2014.115
24. Gamsjaeger S, Masic A, Roschger P et al (2010) Cortical bone composition and orientation as a function of animal and tissue age in mice by Raman spectroscopy. Bone 47:392–399. https://doi.org/10.1016/j.bone.2010.04.608
25. Taylor EA, Lloyd AA, Salazar-Lara C, Donnelly EL (2017) Raman and FT-IR mineral to matrix ratios correlate with physical chemical properties of model compounds and native bone tissue. Appl Spectrosc 71(10):2404–2410. https://doi.org/10.1177/0003702817709286
26. Gamsjaeger S, Robins SP, Tatakis DN et al (2017) Identification of pyridinoline trivalent collagen cross-links by Raman microspectroscopy. Calcif Tissue Int 100(6):565–574. https://doi.org/10.1007/s00223-016-0232-5
27. Beattie JR, Sophocleous A, Caraher MC et al (2019) Raman spectroscopy as a predictive tool for monitoring osteoporosis therapy in a rat model of postmenopausal osteoporosis. J Mater Sci Mater Med 30(2):25. https://doi.org/10.1007/s10856-019-6226-x
28. de Souza RA, Xavier M, da Silva FF et al (2012) Influence of creatine supplementation on bone quality in the OVX rat model: an FT-Raman spectroscopy study. Lasers Med Sci 27(2):487–495. https://doi.org/10.1007/s10103-011-0976-0
29. Boskey A, Mendelsohn R (2005) Infrared analysis of bone in health and disease. J Biomed Opt 10:031102. https://doi.org/10.1117/1.1922927
30. Saito M, Marumo K (2015) Effects of collagen crosslinking on bone material properties in health and disease. Calcif Tissue Int 97(3):242–261. https://doi.org/10.1007/s00223-015-9985-5
31. Bala Y, Seeman E (2015) Bone's material constituents and their contribution to bone strength in health, disease, and treatment. Calcif Tissue Int 97(3):308–326. https://doi.org/10.1007/s00223-015-9971-y
32. Garnero P (2012) The contribution of collagen crosslinks to bone strength. BoneKey Rep 1:182. https://doi.org/10.1038/bonekey.2012.182
33. Gamsjaeger S, Buchinger B, Zoehrer R et al (2011) Effects of one year daily teriparatide treatment on trabecular bone material properties in postmenopausal osteoporotic women previously treated with alendronate or risedronate. Bone 49:1160–1165. https://doi.org/10.1016/j.bone.2011.08.015
34. Boskey AL, Spevak L, Weinstein RS (2009) Spectroscopic markers of bone quality in alendronate-treated postmenopausal women. Osteoporos Int 20:793–800. https://doi.org/10.1007/s00198-008-0725-9
35. Durchschlag E, Paschalis EP, Zoehrer R et al (2006) Bone material properties in trabecular bone from human iliac crest biopsies after 3- and 5-year treatment with risedronate. J Bone Miner Res 21:1581–1590. https://doi.org/10.1359/jbmr.060701
36. Gamsjaeger S, Buchinger B, Zwettler E et al (2011) Bone material properties in actively bone-forming trabeculae in postmenopausal women with osteoporosis after three years of treatment with once-yearly zoledronic acid. J Bone Miner Res 26:12–18. https://doi.org/10.1002/jbmr.180
37. Gallant MA, Brown DM, Hammond M et al (2015) Bone cell-independent benefits of raloxifene on the skeleton: a novel mechanism for improving bone material properties. Bone 61:191–200. https://doi.org/10.1016/j.bone.2014.01.009.Bone
38. Roschger P, Lombardi A, Misof BM et al (2010) Mineralization density distribution of postmenopausal osteoporotic bone is restored to normal after long-term alendronate treatment: qBEI and sSAXS data from the fracture intervention trial long-term extension (FLEX). J Bone Miner Res 25:48–55. https://doi.org/10.1359/jbmr.090702
39. Ou-Yang H, Paschalis EP, Mayo WE et al (2001) Infrared microscopic imaging of bone: spatial distribution of $CO_3^{(2-)}$. J Bone Miner Res 16:893–900. https://doi.org/10.1359/jbmr.2001.16.5.893
40. Donnelly E, Meredith DS, Nguyen JT et al (2012) Reduced cortical bone compositional heterogeneity with bisphosphonate treatment in postmenopausal women with intertrochanteric and subtrochanteric fractures. J Bone Miner Res 27:672–678. https://doi.org/10.1002/jbmr.560
41. Shah FA, Stoica A, Cardemil C, Palmquist A (2017) Multiscale characterisation of cortical bone composition, microstructure, and nanomechanical properties in experimentally-induced osteoporosis. J Biomed Mater Res 106(4):997–1007. https://doi.org/10.1002/jbm.a.36294
42. Miyagawa K, Kozai Y, Ito Y et al (2011) A novel underuse model shows that inactivity but not OVX determines the deteriorated material properties and geometry of cortical bone in the tibia of adult rats. J Bone Miner Metab 29(4):422–436. https://doi.org/10.1007/s00774-010-0241-9
43. Paolillo FR, Romano RA, de Matos L et al (2018) Short-term and long-term effects of osteoporosis on incisor teeth and femoral bones evaluated by Raman spectroscopy and energy dispersive X-ray analysis in OVX rats. J Bone Miner Metab 37(1):18–27. https://doi.org/10.1007/s00774-018-0903-6
44. Paschalis EP, Gamsjaeger S, Condon K, Klaushofer K, Burr D (2019) Estrogen depletion alters mineralization regulation mechanisms in an OVX monkey animal model. Bone 120:279–284. https://doi.org/10.1016/j.bone.2018.11.004
45. Paschalis EP, Gamsjaeger S, Hassler N, Klaushofer K, Burr D (2017) Ovarian hormone depletion affects cortical bone quality differently on different skeletal envelopes. Bone 95:55–64. https://doi.org/10.1016/j.bone.2016.10.029
46. Gourion-Arsiquaud S, Burket JC, Havill LM et al (2009) Spatial variation in osteonal bone properties relative to tissue and animal age. J Bone Miner Res 24:1271–1281. https://doi.org/10.1359/jbmr.090201
47. Qing H, Ardeshirpour L, Pajevic PD et al (2012) Remodeling in mice during lactation. J Bone Miner Res 27:1018–1029. https://doi.org/10.1002/jbmr.1567
48. Kaya S, Basta-Pljakic J, Seref-Ferlengez Z et al (2017) Lactation-induced changes in the volume of osteocyte lacunar-canalicular space alter mechanical properties in cortical bone tissue. J Bone Miner Res 32:676–680. https://doi.org/10.1002/jbmr.3090
49. Bonewald LF, Johnson ML (2008) Osteocytes, mechanosensing and Wnt signaling. Bone 42:606–615. https://doi.org/10.1016/j.bone.2007.12.224
50. Rath Bonivtch A, Bonewald LF, Nicolella DP (2007) Tissue strain amplification at the osteocyte lacuna: a microstructural finite element analysis. J Biomech 40:2199–2206. https://doi.org/10.1016/j.jbiomech.2006.10.040
51. Lane NE, Yao W, Balooch M et al (2006) Glucocorticoid-treated mice have localized changes in trabecular bone material properties and osteocyte lacunar size that are not observed in placebo-treated or estrogen-deficient mice. J Bone Miner Res 21:466–476. https://doi.org/10.1359/JBMR.051103
52. Baylink DJ, Wergedal JE (1971) Bone formation by osteocytes. Am J Physiol 221:669–678

53. Villanueva AR, Ramser JR, Frost HM et al (1966) Tetracycline-based quantitative measurements of the tissue and cell dynamics in 10 cases of osteoporosis. Clin Orthop Relat Res 46:203–217
54. Frost HM (1969) Tetracycline-based histological analysis of bone remodeling. Calcif Tissue Res 3:211–239